Applied Physics Letters

Through-substrate terahertz time-domain reflection spectroscopy for environmental graphene conductivity mapping

Cite as: Appl. Phys. Lett. **116**, 021105 (2020); https://doi.org/10.1063/1.5135644
Submitted: 07 November 2019 . Accepted: 23 December 2019 . Published Online: 16 January 2020

Hungyen Lin, Oliver J. Burton, Sebastian Engelbrecht, Kai-Henning Tybussek, Bernd M. Fischer, and Stephan Hofmann

Applied Physics Letters ARTICLE scitation.org/journal/apl

Through-substrate terahertz time-domain reflection spectroscopy for environmental graphene conductivity mapping

Cite as: Appl. Phys. Lett. **116**, 021105 (2020); doi: 10.1063/1.5135644
Submitted: 7 November 2019 · Accepted: 23 December 2019 ·
Published Online: 16 January 2020

Hungyen Lin,[1,a)] Oliver J. Burton,[2] Sebastian Engelbrecht,[3] Kai-Henning Tybussek,[3] Bernd M. Fischer,[3] and Stephan Hofmann[2]

AFFILIATIONS

[1]Department of Engineering, Lancaster University, Lancaster LA1 4YW, United Kingdom
[2]Department of Engineering, University of Cambridge, J. J. Thomson Avenue, Cambridge CB3 0FA, United Kingdom
[3]French-German Research Institute of Saint-Louis, Saint-Louis 68301, France

[a)]Author to whom correspondence should be addressed: h.lin2@lancaster.ac.uk

ABSTRACT

We demonstrate how terahertz time-domain spectroscopy (THz-TDS) operating in reflection geometry can be used for quantitative conductivity mapping of large area chemical vapor deposited graphene films through silicon support. We validate the technique against measurements performed using the established transmission based THz-TDS. Our through-substrate approach allows unhindered access to the graphene top surface and thus, as we discuss, opens up pathways to perform *in situ* and in-operando THz-TDS using environmental cells.

Significant progress has been made in the crystal growth of 2D materials, particularly for graphene where large-area, highly crystalline mono-layer films can now routinely be produced by chemical vapor deposition (CVD).[1–5] For scaled graphene manufacturing and many emerging device applications, often not growth itself but adequate characterization and quality control of the graphene films have become the key challenge.[6,7] Among a range of emerging contactless electrical characterization methods,[6] terahertz time-domain spectroscopy (THz-TDS) operating in transmission geometry has demonstrated to accurately map the conductivity and mobility of graphene over large areas, producing data consistent with the Drude model to describe graphene intra-band transitions.[8–13] Graphene's complex conductivity is determined by the THz pulse transmitted through the graphene film relative to the support and analyzed using Fresnel coefficients where graphene is modeled as an infinitely thin conducting film. Drift and field-effect mobilities can then be extracted by fitting the conductivity spectra to the Drude model[14] and measuring conductivity changes in response to back-gate voltages,[15] respectively. By repeating the measurement and analysis across the entire graphene area, a conductivity or mobility map can be reliably produced. Measurements have since been extended to reflection geometry[16,17] because (1) limited power can be generated with currently available pulsed THz sources; (2) scenarios that prohibit a direct line-of-sight measurement.

In this Letter, we demonstrate reflection-based THz-TDS of graphene through the supporting substrate. We show that this approach allows us to maintain the previously established contactless mapping capabilities, while giving unhindered access to the graphene top surface and thus opening up pathways to perform *in situ* and in-operando THz-TDS using environmental cells. We employ Si wafers not only as the support for CVD graphene films but also as the window to an environmental cell and, as proof of principle, show that graphene conductivity changes based on different gas environments can be straightforwardly measured by this approach. We validate the technique against current state-of-the-art THz-TDS transmission measurements and demonstrate close agreement between the conductivity histograms for different graphene samples. We discuss many future possibilities that this approach opens ranging from gas- and biosensor development to fast, non-contact, wafer scale correlative probing combined for instance with imaging ellipsometry.[18]

As the reference process and material, we use well-established graphene CVD on commercial Cu foil and subsequent PMMA (poly methyl-methacrylate) transfer[19,20] for which we developed well calibrated processes.[2,3] We use standard Cu foils (25 μm thick, Alfa Aesar purity 99.8%) and CH_4 as the carbon precursor.[2] For transfer, PMMA was used as the support, followed by $(NH_4)_2S_2O_8$ chemical etching to remove Cu. As the target substrate, we used float-zone Si wafers

(1000 ± 25 μm thick) because of low dispersion and absorption properties in the far-infrared range.[21] Raman spectroscopy was performed using a 532 nm laser for characterizing the transferred graphene.

Reflection-based THz-TDS experiments were conducted using a TeraFlash system (Toptica, Munich, Germany), shown in Fig. 1. The THz radiation used here is broadband, covering a spectral range of 0.15–3 THz in free-space, and is generated by pumping a biased photoconductive antenna with an ultrashort laser pulse from a femtosecond laser operating at 1560 nm. The emitted THz pulse is collected and collimated by a parabolic mirror of focal length 101.16 mm where a portion of the generated THz pulse is transmitted through a 3 mm thick high resistivity silicon wafer, which functions as a beam splitter, and is focused onto the sample at normal incidence by another parabolic mirror. The reflected pulse is then partly reflected by the silicon wafer and detected by the detector via a third parabolic mirror. Such a reflection system achieves a THz beam diameter of approximately 1.2 mm at 1 THz. One of the main barriers for accurately extracting optical parameters in reflection is the sensitivity to phase misalignment between the sample and reference measurements. This requirement is mitigated by using first (air-substrate) and second (substrate-graphene-air) reflections as reference and sample signals, respectively.[22] Given the substrate refractive index and Tinkham's formulas for thin conducting films,[23] the equation for obtaining complex conductivity from the reflection measurements at normal incidence in free-space using plane wave approximation can be derived as

$$\tilde{\sigma} = \frac{\left(n_s(A^2-1) + A^2 + 2A\cos\varnothing + 1\right) - j(2An_s\sin\varnothing)}{z_0(1 + A^2 + 2A\cos\varnothing)}, \quad (1)$$

where $Ae^{j\varnothing} = \frac{\tilde{r}\rho_{as}\exp\left(\frac{j2n_s\omega l}{c}\right)}{\tau_{as}\tau_{sa}}$, with $\tilde{r}$ being the Fourier transformed ratio between the reflected wave's complex electric field from the sample to the reference of refractive index n_s and thickness l. Other parameters such as ρ_{as}, τ_{as}, and τ_{sa} correspond to Fresnel's reflection ρ and transmission τ coefficients, where the subscripts indicate the dielectric interfaces: air (a) and substrate (s). ω is the angular frequency, c is the speed of light in vacuum, and z_0 is the vacuum impedance (376.7 Ω). The use of plane wave approximation is valid in Eq. (1) because of a relatively low numerical aperture (~0.25). Such approximations were also used for analyzing transmission measurements,[8,24] which have been validated using micro four-point probe measurements.[8] Analytical simulation was then performed to validate the derived expression and additionally provided a means to investigate the effect of varying substrate thicknesses (several micrometers) on the graphene's complex conductivity spectra,[16] which can then be corrected by iteratively multiplying a phase shift term $\exp\left(\frac{j2n_s\omega\Delta x}{c}\right)$, where Δx corresponds to thickness variation. A similar phase compensation scheme was also demonstrated for transmission.[13] Graphene on the silicon substrate was investigated using a THz spectrometer in Fig. 1 at a step size of 500 μm where 50 waveforms were averaged to represent a measurement for a single pixel under nitrogen purge. As the first reflection was well separated from the second reflection, a time windowing function was used to isolate the acquired waveforms. A spatially averaged conductivity map was subsequently generated by raster scanning the sample and performing the analysis using Eq. (1). In order to validate our proposed method, the same sample was scanned using a THz spectrometer configured in transmission geometry with four off-axis parabolic mirrors. The sample at normal incidence to the incident

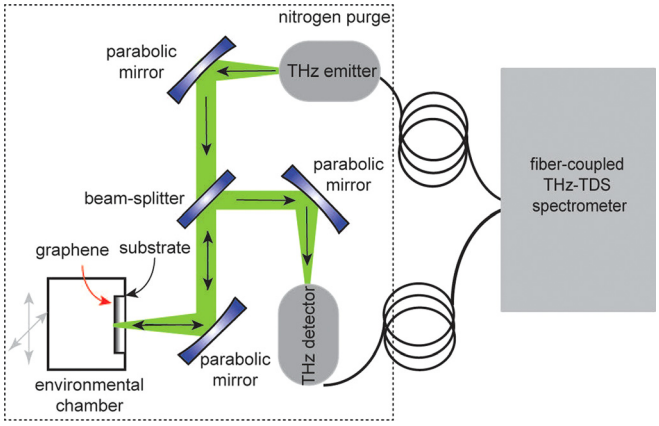

FIG. 1. Schematic of the reflection-based THz-TDS to measure the complex conductivity of graphene through the substrate in a nitrogen purge environment.

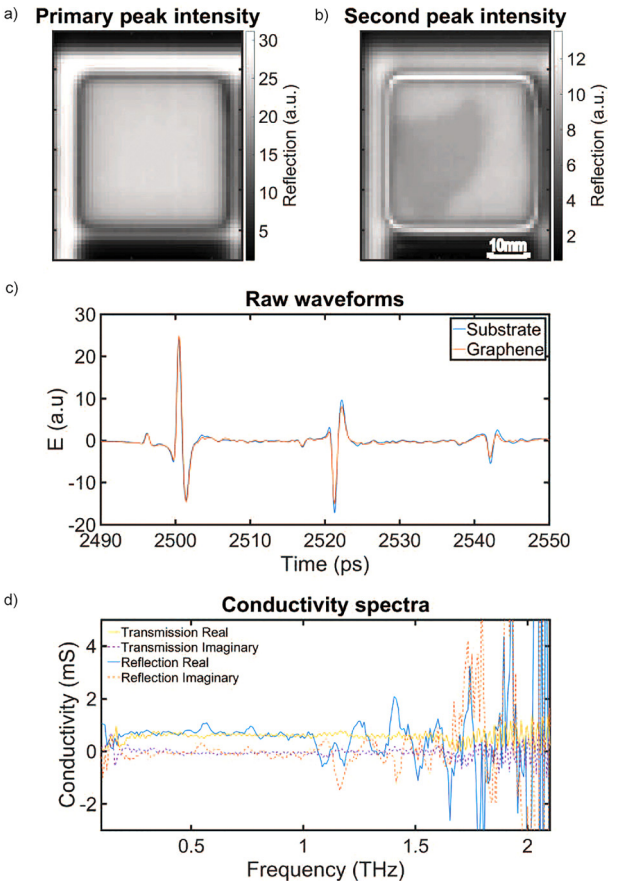

FIG. 2. Primary (a) and secondary (b) peak THz intensity maps measured using THz-TDS in reflection geometry through the substrate. The corresponding THz reflection on the substrate and graphene in (c) in order to calculate the graphene's conductivity spectra for comparison against transmission (d).

THz beam was placed at the focus point between two central parabolic mirrors also under nitrogen purge. Data were also acquired at 50 waveform averages at 500 μm step sizes. By performing the analysis detailed in Refs. 8 and 24, a spatially averaged conductivity map for approximately the same area was generated.

Figures 2(a)–2(d) show THz reflections from the graphene sample, with maps showing the primary and secondary peak intensities and waveforms from points on the substrate and graphene. The corresponding Raman 2D/G ratio map [see Figs. S1(a)–S1(c)] shows an average 2D/G ratio of around 4, highlighting that the film is predominately monolayer graphene. As expected, graphene covered areas correspond to regions with attenuated reflected THz intensities relative to the support due to a higher carrier absorption.[24] With the support being sufficiently thick, a series of reflected THz pulses are separated out in the time domain [Fig. 2(c)], where the first and second reflections are used as the reference and sample, respectively. The measured refractive index is 3.2 in close agreement with 3.29 measured using transmission THz-TDS, which is within 5% of the literature value.[21] The slight discrepancy may be due to sample surface related imperfections, leading to scattering losses and measurement using a focused beam as opposed to a collimated beam.[25] These values are then used to calculate graphene's complex conductivity spectra shown using Eq. (1) without any phase correction, where a flat conductivity spectrum can be observed. This spectrum is compared against the conductivity spectrum measured using transmission THz-TDS at a similar graphene location. The small peaks in the reflection spectra at 0.55 THz and 0.75 THz are artifacts caused by water line absorption in ambient air inside the nitrogen purged environment due to a slightly longer THz beam-path with a possibly lower nitrogen flow than the transmission environment. As any phase misalignment would only significantly affect the imaginary part of the conductivity,[13] we place our emphasis only on the real part of the conductivity. As the conductivity spectrum is approximately constant over the spectral range, the representative conductivity is taken as the average between 0.8 and 1 THz to avoid the water absorption lines without the substantial loss to spatial resolution. Figure 3 compares the conductivity map and Gaussian-fitted histogram obtained using the transmission THz-TDS and the proposed method, where a good agreement between the averages of the two measurements can be seen ($\sigma_{trans} = 0.57$ mS, $\sigma_{refl} = 0.60$ mS). As an additional validation, the proposed technique at a reduced spatial resolution was applied to a defective sample with two scratches, to generate conductivity maps between 0.5 and 1 THz (due to the absence of distinct water lines in Fig. S2), where a good agreement between the averages of the two measurements is also observed ($\sigma_{trans} = 0.69$ mS, $\sigma_{refl} = 0.65$ mS). The demonstration of the through-substrate reflection measurement means that conductivity can be reasonably estimated directly from the first transmitted or reflected pulse, as previously demonstrated,[13,16] even if the pulse has already undergone a longer propagation path and through the supporting substrate on a system with a reduced bandwidth and signal intensity (only a maximum 15% of signal intensity will arrive at the detector for a mirror reflection in Fig. 1). Compared to transmission measurements where spatial resolutions are typically on the order of several hundreds of micrometers,[8,24] achieving a comparable or higher spatial resolution through the substrate is more difficult because the beam will refract toward the surface normal at a medium of higher refractive index. The frequency dependent THz beam diameter can be estimated from the focal length of the off-axis mirror and the collimated beam size using Gaussian optics,[26] but this estimate is only reliable if the Rayleigh range of the focusing mirror is greater than the substrate thickness.[27,28]

As the local environment can easily modulate graphene's intrinsic electrical properties upon adsorption, here we demonstrate the potential of the proposed method for resolving conductivity changes induced by ambient conditions. In particular, we performed a measurement without nitrogen purge at a laboratory controlled relative humidity level of approximately 30%–40%. The reasons for doing so without a designated environmental cell in a nitrogen purge environment are (1) it is widely known that polar gases resonate at discrete frequencies in the microwave to infrared spectral ranges, leading to

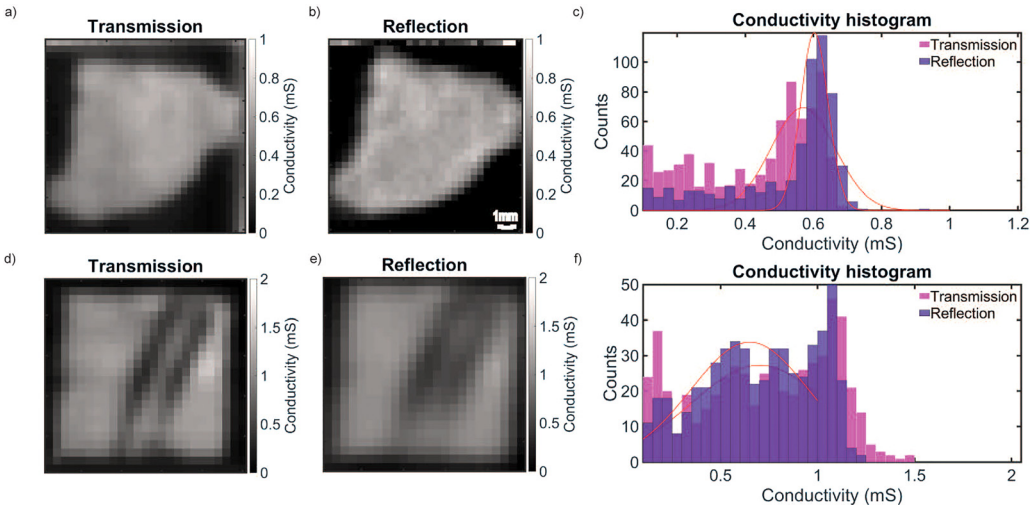

FIG. 3. Conductivity maps of graphene on silicon measured directly using transmission THz-TDS in (a) and (d) and through the substrate in reflection in (b) and (e). The respective conductivity histograms are compared in (c) and (f) with darkened color representing the overlap between the measurements.

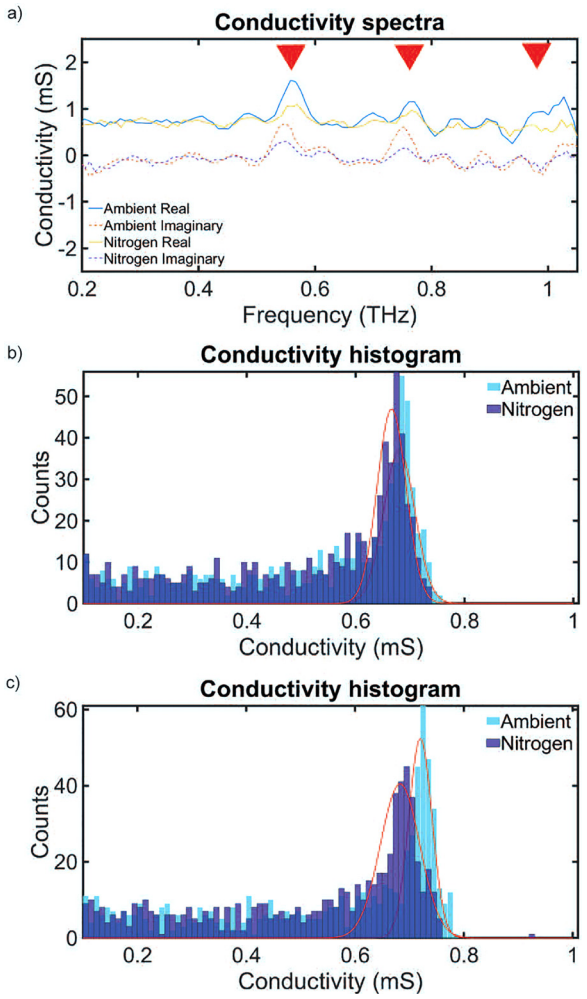

FIG. 4. The complex conductivity spectra determined from measurements acquired at an identical location on the graphene film in the nitrogen and ambient environment (~30%–40% relative humidity), where arrowheads indicate the water vapor lines in (a). By excluding water vapor line contributions, conductivity histograms are compared against the nitrogen environment on different days in (b) and (c) at different relative humidities between 30% and 40%.

sharp resonances corresponding to the transitions between rotational quantum levels, characteristic of the molecular structure;[29] (2) the main constituents of ambient air are nitrogen, oxygen, and water vapor; and (3) remaining polar constituents in the ambient air are observed to have a negligible effect on the THz spectra in the experimental setting (see Fig. S3). Figure 4 compares the complex conductivity spectra of graphene acquired under a nitrogen purge and ambient conditions. As expected, artifacts from the water vapor absorption lines become more pronounced in an ambient condition relative to the nitrogen environment. To quantify the average conductivity change, a representative conductivity is taken as the average between 0.3 and 0.9 THz excluding water vapor line resonances in spectral ranges of 0.5–0.6 THz and 0.7–0.83 THz. The choice to extend the bandwidth from the previous one is to ensure a greater number of data points can be included as part of averaging especially after water vapor line resonances are excluded. These excluded spectral ranges were selected to be sufficiently broad in the case of water line broadening in the unlikely event of pressure or temperature changes. By aggregating conductivity values across the graphene covered areas, the corresponding histogram is generated and compared against the nitrogen purged data. The conductivity averages are then obtained by Gaussian curve-fitting the histograms for the graphene area excluding boundary pixels using the least absolute residual method, resulting in mean values of 0.68 and 0.666 mS for ambient and nitrogen environments, respectively, on one day and mean values of 0.72 and 0.68 mS on another day. This small 2%–5% conductivity increase is at the same order of magnitude but slightly higher than what was reported in an earlier work using direct electrical measurements on a $44 \times 80\ \mu m^2$ patch of CVD graphene on SiO_2/Si wafer support.[30] The slightly higher conductivity reading can be attributed to several factors, such as probing a significantly larger graphene area (at least four orders of magnitude greater) and performing the measurement without a designated environmental cell, thus needing to exclude water vapor contributions. At such a small conductivity change, one also needs to be aware of system's uncertainties, which can be analyzed by comparing the two acquired nitrogen averages resulting in an estimate of 2%. However, this number is likely to be an over-estimate as it assumes a perfect, reproducible nitrogen purge in two days, which in practice is difficult to realize, thus resulting in unintentional doping from other moieties in the ambient air.[31] The fact that the conductivity change is close to previous work[30] is promising and suggests a method of performing *in situ* and in-operando THz-TDS of graphene films inside environmental cells as graphene's electrical conductivity is being modified by the local environment.[31,32] In constructing the cells, even though Si support has been demonstrated, other materials can also be used, provided that they have low dispersion and absorption at THz frequencies.[16,21] Further, the support should be thick enough, with well-polished interfaces, to allow the reflected THz pulses to be well separated in the time domain for temporal windowing. Finally, the medium immersing graphene should satisfy the semi-infinite slab assumption such that subsequent reflections are minimized, resulting in no interference with the medium-graphene-substrate reflection. The immersion medium could be an optically dense dielectric or a thick sample, because an optically dense medium, such as liquid water, will absorb almost all incident THz radiation, while a thick sample will provide sufficient delay for subsequent windowing. By being able to gain an unhindered access to the graphene film, our proposed approach can also be combined with imaging ellipsometry,[18] which could measure graphene directly from an opposing side to the incident THz wave, as part of the correlative probe in order to simultaneously map out electrical conductivity and structural information (layer number, defects, and contamination) at different length scales.

In summary, we have demonstrated the feasibility and potential of measuring the electrical conductivity of CVD graphene through the supporting substrate using THz-TDS in reflection geometry, where the supporting substrate can simultaneously function as a viewing window to an environment designed to modify graphene's electrical properties. Using a THz transparent silicon support, we have validated the proposed technique against a direct measurement using state-of-the-art THz-TDS transmission measurements where there is close agreement between the conductivity histograms for two samples. We have further demonstrated the sensitivity of the technique to resolve

conductivity changes induced by the ambient conditions relative to a nitrogen purged environment, where the resolved changes across large-area graphene are consistent with standard electrical measurements. Our proposed technique opens up the possibility to measure the electrical conductivity of graphene *in situ* without any physical contact, underpinning future continuous macroscopic conductivity monitoring and opening up pathways to perform *in situ* and in-operando THz-TDS using environmental cells. The unhindered nature of the measurement can additionally be used as part of correlative probing to yield simultaneous electrical and structural information.

See the supplementary material for Raman map, conductivity spectra of the defective sample, and magnitude spectrum of silicon reflection in the ambient and nitrogen environment.

H.L. acknowledges financial support from the EPSRC (Grant No. EP/R019460/1). S.H. acknowledges funding from the EPSRC (Grant No. EP/K016636/1, GRAPHTED). We also thank Dr. Philipp Braeuninger-Weimer for useful discussion. Additional data for this article are available at https://doi.org/10.17635/lancaster/researchdata/336.

REFERENCES

[1]S. Bae, H. Kim, Y. Lee, X. F. Xu, J. S. Park, Y. Zheng, J. Balakrishnan, T. Lei, H. R. Kim, Y. I. Song *et al.*, "Roll-to-roll production of 30-inch graphene films for transparent electrodes," Nat. Nanotechnol. **5**(8), 574–578 (2010).
[2]P. Braeuninger-Weimer, B. Brennan, A. J. Pollard, and S. Hofmann, "Understanding and controlling Cu-catalyzed graphene nucleation: The role of impurities, roughness, and oxygen scavenging," Chem. Mater. **28**(24), 8905–8915 (2016).
[3]O. J. Burton, V. Babenko, V. P. Veigang-Radulescu, B. Brennan, A. J. Pollard, and S. Hofmann, "The role and control of residual bulk oxygen in the catalytic growth of 2D materials," J. Phys. Chem. C **123**(26), 16257–16267 (2019).
[4]S. Hofmann, P. Braeuninger-Weimer, and R. S. Weatherup, "CVD-enabled graphene manufacture and technology," J. Phys. Chem. Lett. **6**(14), 2714–2721 (2015).
[5]X. Li, W. Cai, J. An, S. Kim, J. Nah, D. Yang, R. Piner, A. Velamakanni, I. Jung, E. Tutuc *et al.*, "Large-area synthesis of high-quality and uniform graphene films on copper foils," Science **324**(5932), 1312–1314 (2009).
[6]P. Boggild, D. M. A. Mackenzie, P. R. Whelan, D. H. Petersen, J. D. Buron, A. Zurutuza, J. Gallop, L. Hao, and P. U. Jepsen, "Mapping the electrical properties of large-area graphene," 2D Mater. **4**(4), 042003 (2017).
[7]A. C. Ferrari, F. Bonaccorso, V. Fal'ko, K. S. Novoselov, S. Roche, P. Boggild, S. Borini, F. H. L. Koppens, V. Palermo, N. Pugno *et al.*, "Science and technology roadmap for graphene, related two-dimensional crystals, and hybrid systems," Nanoscale **7**(11), 4598–4810 (2015).
[8]J. D. Buron, D. H. Petersen, P. Boggild, D. G. Cooke, M. Hilke, J. Sun, E. Whiteway, P. F. Nielsen, O. Hansen, A. Yurgens *et al.*, "Graphene conductance uniformity mapping," Nano Lett. **12**(10), 5074–5081 (2012).
[9]J. D. Buron, F. Pizzocchero, B. S. Jessen, T. J. Booth, P. F. Nielsen, O. Hansen, M. Hilke, E. Whiteway, P. U. Jepsen, P. Boggild *et al.*, "Electrically continuous graphene from single crystal copper verified by terahertz conductance spectroscopy and micro four-point probe," Nano Lett. **14**(11), 6348–6355 (2014).
[10]C. J. Docherty and M. B. Johnston, "Terahertz properties of graphene," J. Infrared, Millimeter, Terahertz Waves **33**(8), 797–815 (2012).
[11]I. Ivanov, M. Bonn, Z. Mics, and D. Turchinovich, "Perspective on terahertz spectroscopy of graphene," EPL **111**(6), 67001 (2015).
[12]B. Sensale-Rodriguez, R. S. Yan, M. M. Kelly, T. Fang, K. Tahy, W. S. Hwang, D. Jena, L. Liu, and H. G. Xing, "Broadband graphene terahertz modulators enabled by intraband transitions," Nat. Commun. **3**, 780 (2012).
[13]P. R. Whelan, K. Iwaszczuk, R. Wang, S. Hofmann, P. Bøggild, and P. U. Jepsen, "Robust mapping of electrical properties of graphene from terahertz time-domain spectroscopy with timing jitter correction," Opt. Express **25**(3), 2725–2732 (2017).
[14]J. D. Buron, D. M. A. Mackenzie, D. H. Petersen, A. Pesquera, A. Centeno, P. Boggild, A. Zurutuza, and P. U. Jepsen, "Terahertz wafer-scale mobility mapping of graphene on insulating substrates without a gate," Opt. Express **23**(24), 30721–30729 (2015).
[15]J. D. Buron, F. Pizzocchero, P. U. Jepsen, D. H. Petersen, J. M. Caridad, B. S. Jessen, T. J. Booth, and P. Boggild, "Graphene mobility mapping," Sci. Rep. **5**, 12305 (2015).
[16]H. Lin, P. Braeuninger-Weimer, V. S. Kamboj, D. S. Jessop, R. Degl'Innocenti, H. E. Beere, D. A. Ritchie, J. A. Zeitler, and S. Hofmann, "Contactless graphene conductivity mapping on a wide range of substrates with terahertz time-domain reflection spectroscopy," Sci. Rep. **7**, 10625 (2017).
[17]D. M. A. Mackenzie, P. R. Whelan, P. Boggild, P. U. Jepsen, A. Redo-Sanchez, D. Etayo, N. Fabricius, and D. H. Petersen, "Quality assessment of terahertz time-domain spectroscopy transmission and reflection modes for graphene conductivity mapping," Opt. Express **26**(7), 9220–9229 (2018).
[18]P. Braeuninger-Weimer, S. Funke, R. Z. Wang, P. Thiesen, D. Tasche, W. Viol, and S. Hofmann, "Fast, noncontact, wafer-scale, atomic layer resolved imaging of two-dimensional materials by ellipsometric contrast micrography," ACS Nano **12**(8), 8555–8563 (2018).
[19]X. S. Li, L. Colombo, and R. S. Ruoff, "Synthesis of graphene films on copper foils by chemical vapor deposition," Adv. Mater. **28**(29), 6247–6252 (2016).
[20]L. Lin, H. L. Peng, and Z. F. Liu, "Synthesis challenges for graphene industry," Nat. Mater. **18**(6), 520–524 (2019).
[21]D. Grischkowsky, S. Keiding, M. Vanexter, and C. Fattinger, "Far-infrared time-domain spectroscopy with terahertz beams of dielectrics and semiconductors," J. Opt. Soc. Am. B **7**(10), 2006–2015 (1990).
[22]L. Thrane, R. H. Jacobsen, P. U. Jepsen, and S. R. Keiding, "Thz reflection spectroscopy of liquid water," Chem. Phys. Lett. **240**(4), 330–333 (1995).
[23]M. Tinkham, "Energy gap interpretation of experiments on infrared transmission through superconducting films," Phys. Rev. **104**(3), 845–846 (1956).
[24]J. L. Tomaino, A. D. Jameson, J. W. Kevek, M. J. Paul, A. M. van der Zande, R. A. Barton, P. L. McEuen, E. D. Minot, and Y. S. Lee, "Terahertz imaging and spectroscopy of large-area single-layer graphene," Opt. Express **19**(1), 141–146 (2011).
[25]M. Naftaly, "An international intercomparison of THz time-domain spectrometers," in 2016 41st International Conference on Infrared, Millimeter, and Terahertz Waves (IRMMW-THz) (2016).
[26]B. E. A. Saleh and M. C. Teich, *Fundamentals of Photonics*, Wiley Series in Pure and Applied Optics (Wiley, New York, 1991), Vol. xviii, p. 966.
[27]H. Lin, C. Fumeaux, B. M. Fischer, and D. Abbott, "Modelling of sub-wavelength THz sources as Gaussian apertures," Opt. Express **18**(17), 17672–17683 (2010).
[28]H. Lin, C. Fumeaux, B. S. Y. Ung, and D. Abbott, "Comprehensive modeling of THz microscope with a sub-wavelength source," Opt. Express **19**(6), 5327–5338 (2011).
[29]D. M. Mittleman, R. H. Jacobsen, R. Neelamani, R. G. Baraniuk, and M. C. Nuss, "Gas sensing using terahertz time-domain spectroscopy," Appl. Phys. B **67**(3), 379–390 (1998).
[30]A. D. Smith, K. Elgammal, F. Niklaus, A. Delin, A. C. Fischer, S. Vaziri, F. Forsberg, M. Rasander, H. Hugosson, L. Bergqvist *et al.*, "Resistive graphene humidity sensors with rapid and direct electrical readout," Nanoscale **7**(45), 19099–19109 (2015).
[31]V. Panchal, C. E. Giusca, A. Lartsev, N. A. Martin, N. Cassidy, R. L. Myers-Ward, D. K. Gaskill, and O. Kazakova, "Atmospheric doping effects in epitaxial graphene: Correlation of local and global electrical studies," 2D Mater. **3**(1), 015006 (2016).
[32]F. Schedin, A. K. Geim, S. V. Morozov, E. W. Hill, P. Blake, M. I. Katsnelson, and K. S. Novoselov, "Detection of individual gas molecules adsorbed on graphene," Nat. Mater. **6**(9), 652–655 (2007).